Received: 8 May 2020 | Revised: 15 June 2020 | Accepted: 21 June 2020

DOI: 10.1002/bit.27471

ARTICLE

BIOTECHNOLOGY AND BIOENGINEERING WILEY

On the donor substrate dependence of group-transfer reactions by hydrolytic enzymes: Insight from kinetic analysis of sucrose phosphorylase-catalyzed transglycosylation

Mario Klimacek[1] | Alexander Sigg[1] | Bernd Nidetzky[1,2]

[1]Institute of Biotechnology and Biochemical Engineering, Graz University of Technology, NAWI Graz, Graz, Austria

[2]Austrian Centre of Industrial Biotechnology (acib), Graz, Austria

Correspondence
Bernd Nidetzky, Institute of Biotechnology and Biochemical Engineering, Graz University of Technology, NAWI Graz, Petersgasse 10-12/I, A-8010 Graz, Austria.
Email: bernd.nidetzky@tugraz.at

Funding information
European Commission, Grant/Award Number: 761030 (CARBAFIN)

Abstract

Chemical group-transfer reactions by hydrolytic enzymes have considerable importance in biocatalytic synthesis and are exploited broadly in commercial-scale chemical production. Mechanistically, these reactions have in common the involvement of a covalent enzyme intermediate which is formed upon enzyme reaction with the donor substrate and is subsequently intercepted by a suitable acceptor. Here, we studied the glycosylation of glycerol from sucrose by sucrose phosphorylase (SucP) to clarify a peculiar, yet generally important characteristic of this reaction: partitioning between glycosylation of glycerol and hydrolysis depends on the type and the concentration of the donor substrate used (here: sucrose, α-D-glucose 1-phosphate (G1P)). We develop a kinetic framework to analyze the effect and provide evidence that, when G1P is used as donor substrate, hydrolysis occurs not only from the β-glucosyl-enzyme intermediate (E-Glc), but additionally from a non-covalent complex of E-Glc and substrate which unlike E-Glc is unreactive to glycerol. Depending on the relative rates of hydrolysis of free and substrate-bound E-Glc, inhibition (*Leuconostoc mesenteroides* SucP) or apparent activation (*Bifidobacterium adolescentis* SucP) is observed at high donor substrate concentration. At a G1P concentration that excludes the substrate-bound E-Glc, the transfer/hydrolysis ratio changes to a value consistent with reaction exclusively through E-Glc, independent of the donor substrate used. Collectively, these results give explanation for a kinetic behavior of SucP not previously accounted for, provide essential basis for design and optimization of the synthetic reaction, and establish a theoretical framework for the analysis of kinetically analogous group-transfer reactions by hydrolytic enzymes.

KEYWORDS

glycoside hydrolase, glycoside phosphorylase, hydrolase, kinetic mechanism, transfer reaction

Abbreviations: *Ba*SucP, SucP from *Bifidobacterium adolescentis*; *Lm*SucP, SucP from *Leuconostoc mesenteroides*; E-Glc, β-glucosyl-enzyme intermediate; G1P, α-D-glucose 1-phosphate; GG, α-D-glucosyl-*sn*-glycerol; SucP, sucrose phosphorylase (EC 2.4.1.7).

Mario Klimacek and Alexander Sigg contributed equally for this study.

1 | INTRODUCTION

Many enzymes in enzyme class 3 (hydrolases) catalyze chemical group transfer to acceptors (e.g., alcohols) other than water. Such donor-to-acceptor transfer reactions are the basis for important applications of hydrolytic enzymes in organic synthesis (Adlercreutz, 2017; Giordano, Ribeiro, & Giordano, 2006; Kasche, 1986; Marsden, Mestrom, McMillan, & Hanefeld, 2020; Müller et al., 2020; Seibel, Jördening, & Buchholz, 2006; Vera, Guerrero, Aburto, Cordova, & Illanes, 2020). Commercial-scale production of various chemicals and ingredients (e.g., oligosaccharides and glycosides (van Rantwijk, Woudenberg-van Oosterom, & Sheldon, 1999; Vera et al., 2020), esters and triglycerides (Adlercreutz, 2017; Mestrom, Claessen, & Hanefeld, 2019; Norjannah, Ong, Masjuki, Juan, & Chong, 2016), β-lactam antibiotics (Giordano et al., 2006; Kasche, 1986), phosphorylated nucleosides (Asano, Mihara, & Yamada, 1999; Ishikawa, Mihara, Shimba, Ohtsu, & Kawasaki, 2002; Kato, Ooi, & Asano, 1999)) relies on hydrolase-catalyzed group transfer. Glycoside hydrolases (Adlercreutz, 2017; Seibel et al., 2006; Vera et al., 2020; Zeuner, Jers, Mikkelsen, & Meyer, 2014), lipases (Adlercreutz, 2017; Subileau et al., 2017), amidases (Bruggink, Roos, & de Vroom, 1998; Giordano et al., 2006; Gololobov et al., 1990; Sio & Quax, 2004; Sklyarenko, El'darov, Kurochkina, & Yarotsky, 2015), and phosphatases (Ishikawa et al., 2002; Tasnádi, Staśko, Ditrich, Hall, & Faber, 2020; Wildberger, Pfeiffer, Brecker, & Nidetzky, 2015) are industrial enzymes used in these synthetic processes. Mechanistically, the enzymatic reactions proceed in two catalytic steps via a covalent enzyme intermediate (Gololobov, Borisov, Belikov, & Švedas, 1988; Kasche, 1986; Marsden et al., 2020; Seibel et al., 2006; Zeuner et al., 2014). The first step involves group transfer from the donor substrate to an active-site nucleophile of the enzyme. The enzyme intermediate then reacts with the incoming acceptor (which is water in the canonical hydrolysis reaction) to release the synthetic product (Gololobov et al., 1988, 1990; Huber, Kurz, & Wallenfels, 1976; Kasche, 1986; Marsden et al., 2020; Vera et al., 2020; Youshko, Chilov, Shcherbakova, & Švedas, 2002). Synthesis in an aqueous environment operates in competition with hydrolysis (Adlercreutz, 2017; Giordano et al., 2006; Gololobov et al., 1988; Kasche, 1986; Subileau et al., 2017; Wildberger, Pfeiffer, Brecker, Rechberger, et al., 2015). A minimal kinetic mechanism for enzymatic group transfer is shown in Figure 1. The mechanism implies that synthesis and hydrolysis product are formed in a ratio determined by enzyme selectivity but independent of the donor substrate used (Adlercreutz, 2017; Kasche, 1986; Marsden et al., 2020; Youshko et al., 2002).

The natural moisturizer α-D-glucosyl-*sn*-glycerol (GG), produced industrially using glycosylation of glycerol catalyzed by sucrose phosphorylase (SucP; Bolivar, Luley-Goedl, Leitner, Sawangwan, & Nidetzky, 2017; Goedl, Sawangwan, Mueller, Schwarz, & Nidetzky, 2008; Luley-Goedl, Sawangwan, Mueller, Schwarz, & Nidetzky, 2010), represents a number of hydrolase-promoted transfer reactions for which the reaction scheme shown in Figure 1 is likely an oversimplification (e.g., Fernandez-Lafuente, Rosell, & Guisan, 1998; Gololobov et al., 1988, 1990; Kasche, 1986; Terreni et al., 2005; Vera, Guerrero, Wilson, & Illanes, 2017; Youshko et al., 2002). The SucP can use sucrose (**1**) or G1P (**2**) as donor for GG (**3**) formation (Goedl, Sawangwan, et al., 2008; Goedl, Schwarz, Minani, & Nidetzky, 2007; Renirie, Pukin, van Lagen, & Franssen, 2010). However, the ratio between GG and glucose (hydrolysis product) is ~1.5–2.5-fold higher for transfer from sucrose as compared to transfer from G1P, inconsistent with Figure 1 (Goedl, Sawangwan, et al., 2008). This study was conceptualized to achieve clarification. We considered that mechanistic insight into the donor substrate dependence of the enzymatic glucosyl transfer is fundamentally important, and can be practically significant, in a broad field of applied bio-catalysis using hydrolase enzymes for synthesis (Adlercreutz, 2017; Giordano et al., 2006; Kasche, 1986; Marsden et al., 2020; van Rantwijk et al., 1999).

We studied two SucP enzymes, from *Leuconostoc mesenteroides* (*Lm*SucP; Goedl et al., 2007; Goedl, Schwarz, Mueller, Brecker, & Nidetzky, 2008; Luley-Goedl & Nidetzky, 2010) and *Bifidobacterium adolescentis* (*Ba*SucP; Mirza et al., 2006; van den Broek et al., 2004). Both enzymes have been well characterized previously (Franceus & Desmet, 2020; Goedl, Sawangwan, Wildberger, & Nidetzky, 2010; Goedl, Schwarz, et al., 2008), and the *Lm*SucP is used for commercial production of GG (Luley-Goedl et al., 2010). Guided by kinetic framework analysis developed here, we show that in enzymatic reactions with G1P, hydrolysis takes place not only from the covalent glucosyl-enzyme intermediate (E-Glc), but additionally from a non-covalent complex of E-Glc and G1P which unlike E-Glc cannot be intercepted by glycerol. At G1P concentrations too low for substrate-bound E-Glc to form, the transfer/hydrolysis ratio increases to a value consistent with reaction exclusively through E-Glc, independent of the donor substrate used. Besides explaining kinetic behavior of SucP not previously accounted for (Goedl, Sawangwan,

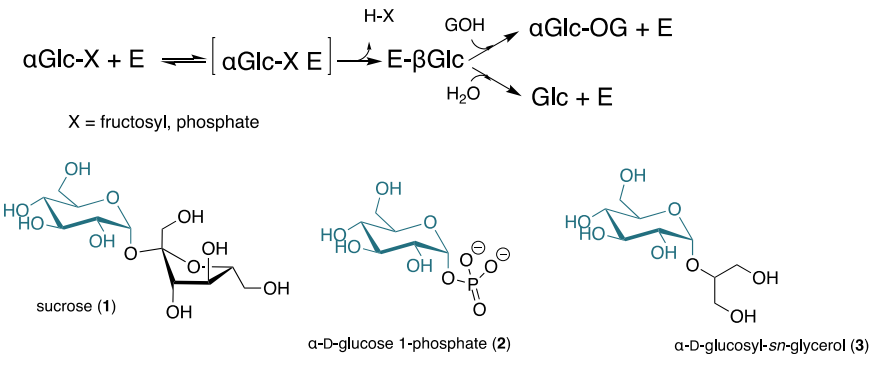

FIGURE 1 Simplified kinetic scheme for SucP-catalyzed synthesis of α-D-glucosyl-*sn*-glycerol (3; GlcOG) via transglucosylation from a glucosyl donor (GlcX) to glycerol (GOH). The donor can be sucrose (**1**) or α-D-glucose 1-phosphate (**2**). X is the leaving group [Color figure can be viewed at wileyonlinelibrary.com]

et al., 2008; Renirie et al., 2010), these results are useful to facilitate model-based optimization of GG synthesis. In addition, our findings expand the theoretical basis for analyzing kinetically analogous group-transfer reactions by hydrolytic enzymes (e.g., Adlercreutz, 2017; Ishikawa et al., 2002; Kasche, 1986).

2 | MATERIALS AND METHODS

2.1 | Materials and enzymes used

Unless noted, the materials used were reported previously (Goedl et al., 2007). *Lm*SucP (GenBank identifier BAA14344) and *Ba*SucP (GenBank identifier AF543301.1) were isolated from *Escherichia coli* overexpression cultures according to literature (Goedl et al., 2007). Their specific activities (phosphorolysis of sucrose) were 166 U/mg (*Lm*SucP) and 108 U/mg (*Ba*SucP), consistent with previous studies (Goedl et al., 2007; van den Broek et al., 2004). Protein was measured with the Bradford assay referenced against BSA.

2.2 | Initial rate studies

Initial reaction rates were obtained in duplicates at 30°C in 50 mM MES buffer, pH 7.0. The protein concentration was 1–3 µg/ml. One substrate concentration (donor, glycerol) was varied, the other was constant at the desired/possible degree of saturation. When analyzing hydrolysis only, no glycerol was present. Samples, typically 5, were taken between 5 and 40 min. Samples were immediately quenched in the same volume of reaction buffer preheated to 99°C and further boiled for 10 min in a water bath.

The glucose released was measured based on a hexokinase/glucose 6-phosphate dehydrogenase assay (Goedl et al., 2007; Klotzsch & Bergmeyer, 1965). The fructose released was determined with essentially the same assay, adding phospho-glucose isomerase (Klotzsch & Bergmeyer, 1965). Detailed protocols for glucose and fructose determination are summarized in the Supporting Information materials and methods section. Phosphate was analyzed with a colorimetric assay (Goedl et al., 2007).

Initial rates were determined from linear time courses of product release. Kinetic parameters were obtained from nonlinear least-square fits (Sigma Plot 10.0) of the data with Equations (1)–(4). Note that the equations used are phenomenological and had the purpose of fitting a single set of data. Equations derived from mechanistic models are shown in Table S1. An important test for quality and consistency of the mechanistic models was to assess their ability to reproduce the results of "phenomenological fits." In Equations (1)–(4), ν_X (s^{-1}), ν_{GG} (s^{-1}), and ν_H (s^{-1}) are the initial rates of the donor substrate consumption measured as release of the leaving group X (= fructose or phosphate), GG release, and hydrolysis, respectively. ν_H was recorded in the presence and absence of glycerol. Note: ν_X is the sum of ν_{GG} and ν_H. [GlcX] and [GOH] are the donor and glycerol concentration, respectively. Throughout this study, initial rates were obtained from volumetric rates (µmol·ml^{-1}·s^{-1}) divided by molar enzyme concentration. The molar concentration is determined from the protein concentration, using a molecular mass of 55 kDa for *Lm*SucP (Goedl et al., 2007) and 56 kDa for *Ba*SucP (Sprogøe et al., 2004). $^{app}V_X$ is an apparent maximum rate constant and ^{app}K an apparent Michaelis constant, while $^{app}K_i$ is an apparent substrate inhibition constant. The transfer coefficient (TC) indicates the rate ratio's (ν_{GG}/ν_H) dependency on [GOH]:

$$\nu_X = \frac{[GlcX]\,{}^{app}V_X}{{}^{app}K_{GlcX} + [GlcX]}, \tag{1}$$

$$\nu_X = \frac{[GlcX]\,{}^{app}V_X}{{}^{app}K_{GlcX} + [GlcX] + \frac{[GlcX]^2}{{}^{app}K_{i,GlcX}}} \tag{2}$$

$$\nu_X = \frac{[GOH]\,{}^{app}V_X}{{}^{app}K_{GOH} + [GOH]} + \nu_H^{[GOH]=0}, \tag{3}$$

$$\frac{\nu_X}{\nu_H} = \frac{\nu_{GG}}{\nu_H} + 1 = TC\cdot[GOH] + 1. \tag{4}$$

2.3 | Kinetic models

The King-Altman open-access tool (http://www.biokin.com/tools/king-altman/index.html) was used to derive mathematical equations for the kinetic schemes described in Section 3. Differential equations have the general form, $\nu = N/D = d[X]/dt$. The numerator (N) and denominator (D) contain coefficients (derived according to fundamental principles of enzyme kinetic theory [Segel, 1993]) that group together the microscopic rate constants into kinetic parameters. For each kinetic scheme, an equation was additionally derived from the rate constants to express the dependence of the rate ratio on the glycerol concentration. A nomenclature is used in which microscopic rate constants for forward and reverse direction of reaction are indicated as k_{+i} and k_{-i}, with i indicating the step in the reaction sequence. Net rate constants (Cleland, 1975) are also used and indicated as k'.

For data fitting, the Microsoft Excel 2019 add-in Solver was used. To determine estimates of each microscopic rate constant, dependencies of ν_X (on [GlcX]), ν_X (on [GOH]) and ν_X/ν_H (on [GOH]) were fitted simultaneously by maximizing the sum of respective coefficients of determination R^2. Dependency of ν_H on [GOH] was used to check quality and consistency of the estimated parameters. Constraints on the microscopic rate constants were derived from experimental (apparent) kinetic parameters of *Lm*SucP and their use is described in Tables S2–S4. Upper and lower boundaries for *Ba*SucP rate constants were reasonably chosen for k_{-3} (Goedl, Sawangwan, et al., 2008).

3 | RESULTS

3.1 | Kinetic scenarios for SucP-catalyzed transglycosylation

To account for a transfer to hydrolysis rate ratio (ν_X/ν_H) dependent on the donor substrate used, we considered possible extensions of

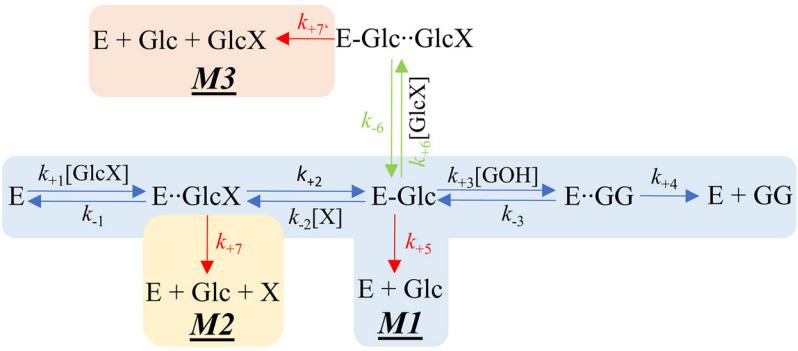

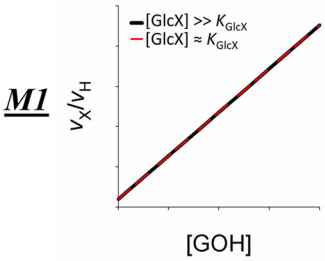

$$\frac{v_X}{v_H} = \frac{k_{+3}k_{+4}}{k_{+5}(k_{-3}+k_{+4})}[GOH] + 1 \quad (5)$$

$$v_H^{[GOH]=0} = \frac{V_H[GlcX]}{[GlcX]+K_{GlcXH}+\frac{[GlcX]^2}{K_{i,GlcX}}} \quad (6)$$

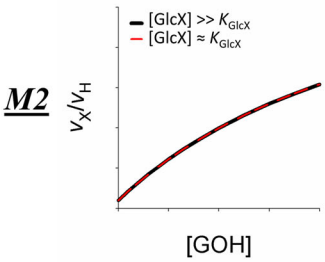

$$\frac{v_X}{v_H} = \frac{k_{+2}k_{+3}k_{+4}[GOH]}{k_{+3}k_{+4}k_{+7}[GOH]+k_{+5}(k_{-3}+k_{+4})(k_{+2}+k_{+7})} + 1 \quad (7)$$

$$\text{... reaches a plateau at } \left(\frac{v_X}{v_H}\right)_{[GOH]=\infty} = \frac{k_{+2}}{k_{+7}} + 1 \quad (8)$$

$$\text{... if } k_{+2} \gg k_{+7};\ \frac{v_X}{v_H} \cong \frac{k_{+3}k_{+4}}{k_{+5}(k_{-3}+k_{+4})}[GOH] + 1 \quad (9)$$

$$v_H^{[GOH]=0} = \frac{V_H[GlcX]}{[GlcX]+K_{GlcXH}+\frac{[GlcX]^2}{K_{i,GlcX}}} \quad (10)$$

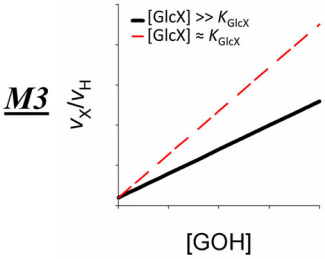

$$\frac{v_X}{v_H} = \frac{k_{+3}k_{+4}[GOH]}{(k_{-3}+k_{+4})\left(k_{+5}+\frac{k_{+6}k_{+7\prime}}{k_{-6}+k_{7\prime}}[GlcX]\right)} + 1 \quad (11)$$

$$\text{... if [GlcX] gets small; } \frac{v_X}{v_H} \cong \frac{k_{+3}k_{+4}}{k_{+5}(k_{-3}+k_{+4})}[GOH] + 1 \quad (12)$$

$$v_H^{[GOH]=0} = \frac{V_H[GlcX]+V_{H2}\frac{[GlcX]^2}{K_{i,GlcX}}}{[GlcX]+K_{GlcXH}+\frac{[GlcX]}{K_{i,GlcX}}K_{GlcXH2}+\frac{[GlcX]^2}{K_{i,GlcX}}} \quad (13)$$

FIGURE 2 Kinetic mechanisms considered in this study and experimentally relevant deductions made from them. V_H and V_{H2} are maximum hydrolysis rates at [GOH] = 0 and glucose is released from E-Glc (mechanisms M1–M3) and additionally from E •• GlcX (mechanism M2) or E-Glc •• GlcX (mechanism M3). K_{GlcXH} and K_{GlcXH2} are binding constants of GlcX to E (mechanisms M1–M3) or E-Glc (mechanism M3). $K_{i,GlcX}$ is an inhibition constant for donor substrate. Microscopic rate constants k_5, k_7, and $k_{+7'}$ include the water concentration dependency and are defined as follows: $k_i = k_i^* \cdot [H_2O]$ [Color figure can be viewed at wileyonlinelibrary.com]

the base mechanism (M1) for enzymatic trans-glycosylation, as shown in Figure 1 and more fully in Figure 2. Mechanism M1 is a canonical Ping-Pong reaction with irreversible release of GG (k_{+4}) and glucose (k_{+5}). Both extensions of mechanism, M2 and M3, assume that not only does hydrolysis occur from E-Glc, but it can also happen from a noncovalent complex of E-Glc, still containing the leaving group expelled from the donor substrate (M2; step k_{+7}) or having a second donor substrate bound (M3; step $k_{+7'}$). While able to undergo hydrolysis, these noncovalent complexes of E-Glc are unreactive towards glycerol. Note: to avoid model complexity not strictly necessary in the analysis, mechanism M2 was formulated to consolidate two chemical reaction steps into one single kinetic step

k_{+7}. One chemical step is the formation of E-Glc with X still bound to the enzyme and the other is hydrolysis of the complex to give free enzyme, glucose, and X. The idea for mechanism M3 arose from experimental evidence of substrate inhibition in the reaction of *Lm*SucP with G1P (see later). Upon hydrolysis, these additional E-Glc complexes can regenerate the free enzyme under release of glucose and the substrate leaving group (M2; k_{+7}) or the substrate (M3; $k_{+7'}$). For each proposed mechanism, we derived mathematical expressions relating the observable kinetic parameters, including ν_X/ν_H (Figure 2), to the microscopic rate constants of the reaction. A detailed summary is given in Table S1. Maximal rate (V) and binding (K) parameters for formation of GG (V_X, K_{GlcX}, K_{GOH}) and hydrolysis (V_H, K_{GlcXH}) are thus defined (Table S1; Figure 2, Equations 5, 7, 11). Substrate inhibition ($K_{i,GlcX}$) is included in all mechanisms. Mechanism M3 involves additional parameters for hydrolysis (V_{H2}) and substrate binding (K_{GlcXH2}), arising from donor substrate binding to the E-Glc intermediate and hydrolysis via step $k_{+7'}$. With the help of these expressions (Figure 2), important deductions can be made for the experiment, which we then show, enable clear-cut mechanistic discrimination.

In particular as demonstrated in Figure 2, mechanism M2 predicts ν_X/ν_H to exhibit curved dependence on [GOH] (Equation (7)), whereas in mechanism M1 ν_X/ν_H increases linearly with [GOH] (Equation (5)). The dependence of ν_X/ν_H on [GOH] derived from mechanism M3 is also linear (Equation (11)). However, contrary to the other mechanisms, mechanism M3 involves a unique effect of the donor substrate concentration [GlcX] on ν_X/ν_H dependent on [GOH], as can be easily realized from the denominator term in Equation (11). The ν_X/ν_H increases when the donor concentration decreases, approaching a limiting value described by Equation (12). Moreover, Equation (7) (mechanism M2) and Equation (11) (mechanism M3) involve rate constants from donor substrate-dependent steps, with the important implication that the ν_X/ν_H for these mechanisms can exhibit dependence on the type of donor substrate used. Equation (5) for mechanism M1, in contrast, involves only rate constants from steps after the E-Glc intermediate, thus requiring the ν_X/ν_H to be independent of the donor used. In mechanism M2, the ν_X/ν_H curve described by Equation (7) reaches plateau at high [GOH], with a maximum value equal to (k_{+2}/k_{+7} + 1) (Equation (8)). In the case that release of X (k_{+2}) is considerably faster than the hydrolysis according to step k_{+7}, Equation (7) reduces to Equation (9) and M2 can no longer be distinguished from M1. Besides its unique feature of ν_X/ν_H dependent on the donor substrate concentration, as shown in Figure 2, mechanism M3 can additionally involve a characteristic deviation from Michaelis-Menten behavior when initial rates dependent on the donor substrate concentration are recorded in the absence of glycerol (cf. Equation (13) (M3) with Equation (6) (M1) and Equation (10) (M2)). Various scenarios are possible from Equation (13): one is inhibition at high [GlcX]; another is that the initial-rate does not reach saturation at high [GlcX]. Both have relevance for the enzymatic reactions, as shown later.

3.2 | Mechanistic analysis of the SucP-catalyzed transglycosylation

Guided by the mathematical deductions from Figure 2, we carried out extensive initial-rate studies for *Lm*SucP and *Ba*SucP, to obtain experimental evidence suitable to achieve mechanistic discrimination. In particular, dependencies on [GlcX] were measured with glycerol present for ν_X or absent for ν_X and ν_H. Dependencies on [GOH] were measured for ν_X, ν_H, and ν_X/ν_H. Donor substrate was saturating (sucrose: 20 mM, both enzymes; G1P: 50 mM, *Lm*SucP; 450 mM, *Ba*SucP). Using G1P, approximately half-saturating concentration was additionally applied (5 mM, *Lm*SucP; 50 mM; *Ba*SucP). The experimental data are shown together with the results of best-model fits in Figure 3 (*Lm*SucP) and Figure S2 (*Ba*SucP).

3.2.1 | Analysis of the *Lm*SucP reaction

Reaction of *Lm*SucP with sucrose and glycerol is described very well by the base mechanism M1 (see the values of R^2 in Figure 3 Panels a1 –e1). Dependence of ν_X on [Suc] is of the Michaelis-Menten type, with a K_{GlcXH} that increases to K_{GlcX} when glycerol is present, as expected. Dependence of ν_X on [GOH] is a straight line as is the dependence of ν_X/ν_H on [GOH]. The ν_H is largely unaffected by [GOH], and the experimental dependence is reproduced in excellent quality by the model with parameters estimated from the data in Figure 3 Panels a1,b1,c1,e1.

Using G1P (50 mM) as the donor, the transfer coefficient from the dependence of ν_X/ν_H (TC = 3.3 ± 0.1 M^{-1}; determined from linear regression of the data) was 1.4-fold smaller than the TC (= 4.7 ± 0.1 M^{-1}) obtained from the corresponding ν_X/ν_H dependence using sucrose as the donor (Figure 3 Panel e1). Mechanism M1 is unable to account for this difference. Best fits based on mechanism M2 required that k_{+7} be effectively zero. For conditions of k_{+7} = 0, mechanism M2 is reduced to mechanism M1 (Figure 2), thus eliminating it from consideration.

Using mechanism M3, excellent fit of the full set of data was obtained, as shown in Figure 3 Panels a2–e2. Characteristic features of the reaction are captured precisely: the substrate inhibition by G1P (Figure 3 Panel b2) and the dependence of ν_X/ν_H on [GOH]. The internal control (dependence of ν_H on [GOH]) was reproduced very well using parameter estimates from the fit. Most importantly in view of mechanism discrimination, however, mechanism M3 predicts that at low concentrations of G1P (here: 5 mM) that prevent formation of the inhibitory complex between E-Glc and G1P (Figure 2), the dependence of ν_X/ν_H on [GOH] should become close to what it was with sucrose as the donor substrate. The TC determined at 5 mM G1P was 4.8 ± 0.1 M^{-1} (Figure 3 Panel e3) in perfect agreement with the TC obtained from the sucrose data. Mechanism M3 also captured the appearance of curvature in the dependence of ν_X on [GOH] recorded at 5 mM G1P (Figure 3 Panel c3). This was not present in analogous dependencies determined at 50 mM G1P (Figure 3 Panel c2) or using sucrose (Figure 3 Panel c1). Finally, decrease of ν_X at high [GOH] was predicted with excellent accuracy for the conditions of 5 mM G1P.

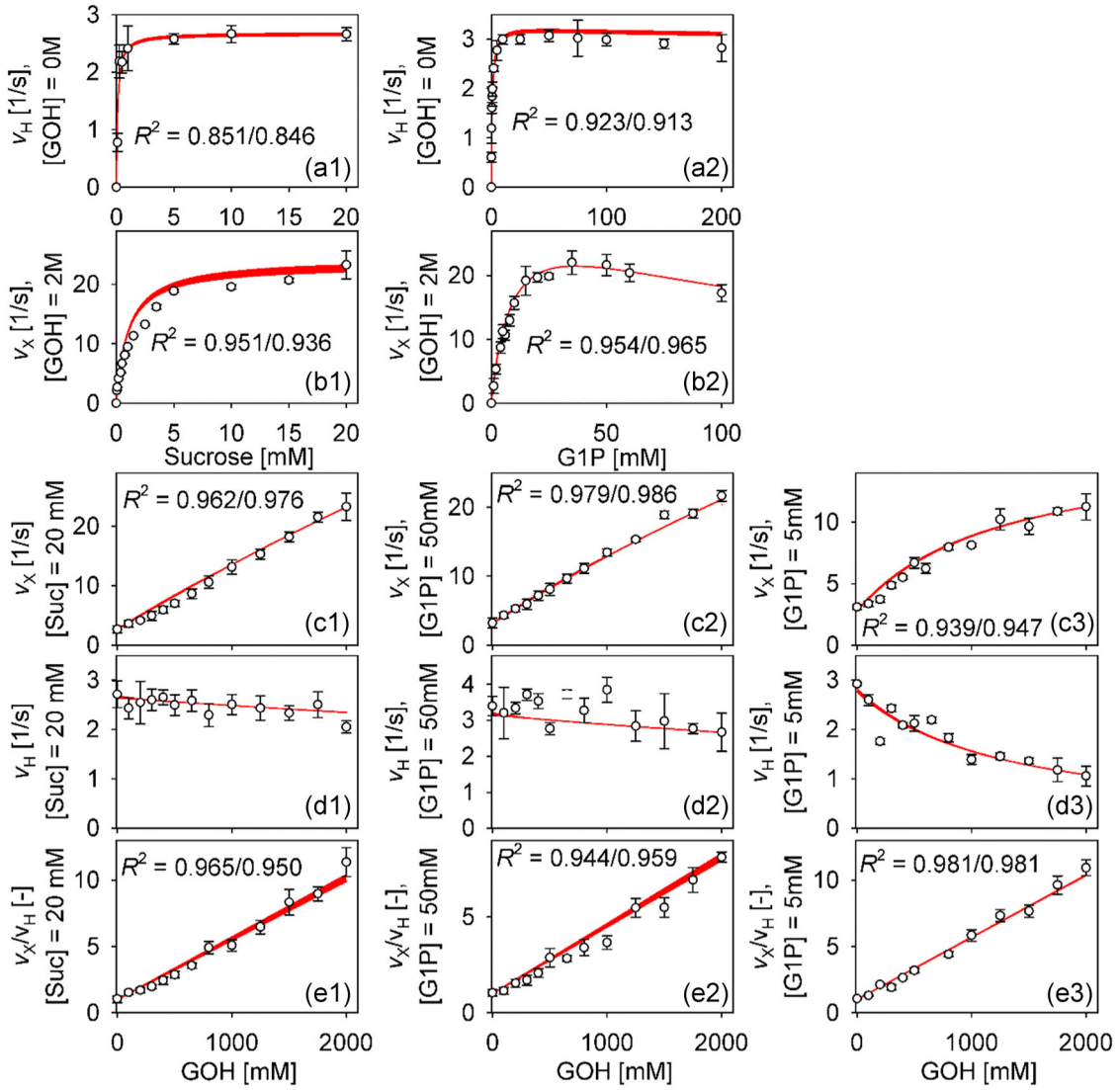

FIGURE 3 Results from fitting kinetic mechanisms M1 and M3 to experimental data for *Lm*SucP-catalyzed the transglucosylation from sucrose (Panels 1) and G1P (Panels 2 and 3), to glycerol. Experimental data are presented as averages (circles) and corresponding standard deviations (error bars). Solution spaces of resultant fits are shown in red. Effect of changing k_{+4} (195.15/10^5 s^{-1}) on R^2 values is shown. Note, that data from Panels (d1) to (d3) were not included in the fitting process and compare calculated hydrolysis rates with experimental data. Initial rates of donor group release (X = fructose or phosphate) are indicated by ν_X in Panels (a), (b), (c) and (e), while those of glucose formation are represented by ν_H in Panels (d) and (e) [Color figure can be viewed at wileyonlinelibrary.com]

Boundaries of first- and second-order rate constants for the enzymatic half-reaction with sucrose or G1P leading up to the E-Glc intermediate can be derived from steady-state apparent kinetic parameters ($^{app}V_X$, $^{app}V_X$, $^{app}K_{GlcX}$) of *Lm*SucP reported in the literature (Mueller & Nidetzky, 2007). Details are given in Tables S2–S4. We assessed the obtained results for consistency by calculating the equilibrium constant (K_{eq}) for the reaction, sucrose + phosphate ↔ fructose + G1P. The K_{eq} values obtained from the model parameters (K_{eq} = 11.3–38.4) are in reasonable agreement with the experimentally determined K_{eq} values of 9 ± 5.5 (Wildberger, Luley-Goedl, & Nidetzky, 2011) and 44 ± 26 (Goedl et al., 2007). Substantial variation in the experimental K_{eq} values has been noted in Wildberger et al. (2011) but the reason for it was not identified.

Rate constants for the half-reaction of E-Glc with glycerol and water must be independent of the donor substrate used. However, high deviation in the rate of GG release (k_{+4}) was observed in the best fit results for sucrose (195.15 s^{-1}) and G1P (>10^5 s^{-1}). Consequently, influence of on fit quality was investigated within the observed lower (195.15 s^{-1}) and upper boundaries (10^5 s^{-1}). The observed solution spaces on kinetic rate constants and kinetic parameters are shown in Tables S5 and S6. The effects on fit quality are shown in Figure 2 (red areas). The glycerol binding constant to E-Glc (k_{+3}) estimated from sucrose (0.013–0.012 s^{-1}·M^{-1}) or G1P data (0.016–0.016 s^{-1}·M^{-1}) was fully consistent. The rate constant for hydrolysis of E-Glc (k_{+5}) was similar as estimated from sucrose (2.72–2.68 s^{-1}) and G1P data (3.37–3.32 s^{-1}). Hydrolysis of the complex of E-Glc and G1P occurred with a similar rate

($k_{+7'}$ = 3.0–3.0 s^{-1}). The complete sets of rate constants and calculated kinetic parameters are summarized in Tables S5 and S6. As shown, fits of the data were rather insensitive to changes in the rate constant for release GG (k_{+4}) (see Figure 3). Constancy of k_{+4} for reaction with sucrose and G1P can thus be assumed. The k_{+4} estimate of 195 s^{-1} obtained from the sucrose data was therefore used in further analyses.

We show in Table 1 that employing the rate constants from Table S5 (k_{+4} = 195 s^{-1}), mechanisms M1 and M3 show excellent capability to reproduce the apparent kinetic parameters of the reaction with sucrose and G1P for given substrate conditions, respectively. This immediately suggests practical utility of the models for prediction and optimization purposes (see Section 4).

3.2.2 | Analysis of the *Ba*SucP reaction

As was the case with *Lm*SucP, the base mechanism M1 provided an excellent description of the reaction of *Ba*SucP with sucrose and glycerol (Figure S2, panels A1–E1). The dependence of ν_X/ν_H on [GOH] showed a 1.7-fold larger slope (= *TC*) for *Ba*SucP compared to *Lm*SucP. The *TC* determined directly from reactions of *Ba*SucP at high and low [G1P] was 6.3 ± 0.1 and 8.1 ± 0.1 M^{-1}, respectively. Evidence that the *TC* was dependent on both the type and the concentration of donor substrate effectively ruled out the applicability of mechanisms M1 and M2.

Fit with mechanism M3 generally yielded useful representations of all subsets of the data (Figure S2, Panels A2–E1 and C3–E3). Peculiarities already noted for reactions of *Lm*SucP, like the dependence of ν_X on [GOH] developing curvature at low [G1P] (Figure S2, Panel C3 compared with Panel C2), were reproduced very well by the model. Despite some disagreement between model and experiment in absolute numbers (hence the relatively small R^2 of 0.804) (Figure 4 Panel a), mechanism M3 nonetheless captured fully the pronounced deviation from Michaelis-Menten behavior in the dependence of ν_H on [G1P] when no glycerol was present. The dependence is biphasic. The initial "high affinity" phase at low substrate concentration (≤4 mM) exhibits a steep increase in ν_H with [G1P]. However, rather than reaching plateau at high substrate concentration, the dependence changes into a second "low-affinity" phase in which ν_H again increases with increasing [G1P], yet at a much shallower slope. The biphasic dependence of ν_H on [G1P] accords very well with

TABLE 1 Apparent kinetic parameters for *Lm*SucP and *Ba*SucP obtained from fits of experimental data and calculated using rate constants for mechanisms M1 and M3

	*Lm*SucP		*Ba*SucP	
	Data fit	**Kinetic mechanism[e]**	**Data fit**	**Kinetic mechanism**
Sucrose, M1				
	[GOH] = 2 M		**[GOH] = 2 M**	
$^{app}V_X$ (s^{-1})	23.3 ± 0.45[a]	23.2	15.9 ± 0.1[a]	15.3
$^{app}K_{Suc}$ (mM)	1.4 ± 0.1[a]	1.0	0.45 ± 0.01[a]	0.46
	[Suc] = 20 mM		**[Suc] = 20 mM**	
$\nu_H^{[GOH]=0}$ (s^{-1})	2.1 ± 0.3[b]	2.68	0.5 ± 0.1[b]	0.88
$^{app}V_X/^{app}K_{GOH}$ ($M^{-1}\cdot s^{-1}$)	10.7 ± 0.2[b]	12.3	7.1 ± 0.1[b]	7.2
TC (M^{-1})	4.7 ± 0.1[c]	4.7	7.9 ± 0.1[c]	8.2
G1P, M3				
	[GOH] = 2 M		**[GOH] = 2 M**	
$^{app}V_X$ (s^{-1})	36 ± 3[d]	28.5	29.2 ± 0.7[a]	25.8
$^{app}K_{i,G1P}$ (mM)	12.5 ± 1.7[d]	7.6	58 ± 5[a]	48.5
$^{app}K_{i,G1P}$ (mM)	106 ± 21[d]	n.d.[f]	none	
	[G1P] = 50 mM		**[G1P] = 450 mM**	
$^{app}V_X$ (s^{-1})	122 ± 48[b]	73.9	144 ± 66[b]	238
ν_H (s^{-1})	3.0 ± 0.3[b]	3.20	1.9 ± 0.4[b]	2.0
$^{app}K_{GOH}$ (M)	11.0 ± 0.5[b]	6.6	9.8 ± 5.4[b]	19.6
$^{app}V_X/^{app}K_{GOH}$ ($M^{-1}\cdot s^{-1}$)	11.1[b]	11.2	14.6[b]	12.1
TC (M^{-1})	3.3 ± 0.1[c]	3.65	6.3 ± 0.1[c]	6.0

[a]Equation (1).
[b]Equation (3).
[c]Equation (4).
[d]Equation (2).
[e]Results were calculated with k_{+4} = 195.15 s^{-1}.
[f]A term representing $^{app}K_{i,G1P}$ in Equation (2) cannot be isolated from the rate equation of M3.

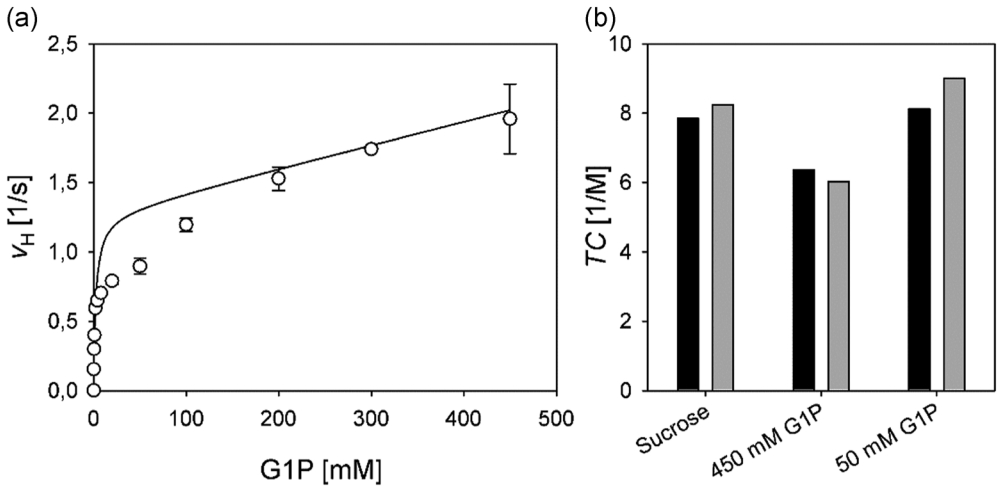

FIGURE 4 Key results of fits of kinetic mechanism M3 to data for *Ba*SucP-catalyzed transglycosylation. (a) Two phasic affinity of G1P to *Ba*SucP determined at 2 M glycerol ($R^2 = 0.804$). (b) Transition transfers obtained by linear regression (intercept = 1.0) of experimental data (black boxes) and estimated by the M1 (sucrose) or M3 (G1P). The complete data set obtained from parameter estimation analysis can be found in Tables S7 and S8

mechanism M3, given that binding constants for high- and low-affinity substrate binding differ by a large amount. Indeed, we estimate from the fits that K_{G1PH2} exceeds K_{G1PH} = 2.4 mM by many orders of magnitude. The apparent "activation" of *Ba*SucP at high [G1P] (Figure 4 Panel a) marks an important distinction between this enzyme and *Lm*SucP which is inhibited by high [G1P] (Figure 3 Panel a2). Large difference in the value of $k_{+7'}$ (*Lm*SucP = 3.0 s^{-1}; *Ba*SucP ≥ 10^3 s^{-1}) is responsible for it. The full set of microscopic rate constants obtained from almost unconstrained fit (only restriction: $0.0 < k_{-3} < 0.0005$ s^{-1}) of mechanism M1 and M3 to the data and the corresponding kinetic parameters are summarized in Tables S7 and S8.

Analogously as with *Lm*SucP, mechanism M3 predicts that, when G1P is used as the donor in reactions of *Ba*SucP, the *TC* will increase with decreasing donor concentration to a limiting value identical with the *TC* of the reaction with sucrose. The experimental data show this *TC* change exactly (Figure 4 Panel b). Other features in which *Ba*SucP is notably different from *Lm*SucP are that hydrolysis of E-Glc is slower by 2.6- to 3.0-fold; in the absence of glycerol, binding to sucrose is 4-fold tighter whereas binding to G1P is 2.6-fold weaker; and the *TC* is ~2-fold higher at all conditions used (donor type and concentration).

4 | DISCUSSION

Using mechanism-based kinetic analysis, we clarify in this study the peculiar behavior of sucrose phosphorylase, that enzyme selectivity for product formation via glycosylation of glycerol and hydrolysis depends on the type and concentration of the glucosyl donor substrate used (Goedl et al., 2007; Goedl, Sawangwan, et al., 2008; Renirie et al., 2010). We present strong evidence for an unanticipated kinetic complex of E-Glc with G1P that can hydrolyze to regenerate the free enzyme upon release of glucose and G1P, but is unable to form the transglycosylation product GG. The molecular interactions involved in the proposed complex are not known in detail. However, it suffices to emphasize that the (acceptor) binding pocket of the E-Glc form of *Ba*SucP is wide and flexible (Mirza et al., 2006; Sprogøe et al., 2004) to accommodate a range of bulky acceptors (Dirks-Hofmeister, Verhaeghe, De Winter, & Desmet, 2015; Goedl et al., 2010; Seibel et al., 2006), including glucose in multiple orientations (Beerens et al., 2017; Kraus, Görl, Timm, & Seibel, 2016; Verhaeghe et al., 2016). The kinetic significance of the (E-Glc •• G1P) complex, in terms of the amount formed at steady state and the rate of breakdown, have strong implications on canonical (apparent) enzyme kinetic parameters obtained from standard experiments (e.g., $^{app}V_X$, ^{app}K, *TC*; see Table 1). The deepened mechanistic understanding obtained from this study enables causes to be related quantitatively to effects and so unifies conflicting evidence from different studies of sucrose phosphorylase (Goedl, Sawangwan, et al., 2008; Renirie et al., 2010) into a coherent whole. The current study comprises two further elements of broad importance. First, the kinetic framework analysis (Figure 2 and the associated algebra in Table S1) provides extended basis for the kinetic evaluation of other hydrolytic enzymes that catalyze chemical group-transfer reactions (e.g., glycosyl, phosphoryl, acyl). As discussed later, there have been numerous studies of such enzymes over decades, but a comprehensive analysis of the different kinetic scenarios surrounding the covalent enzyme intermediate has been worked out only for selected transformations, in particular those of amidases/acyltransferases in β-lactam synthesis (Gololobov et al., 1988, 1990; Schroën et al., 2001; Youshko et al., 2002). Disagreement with the base mechanism M1 has been noted in several instances however (Fernandez-Lafuente et al., 1998; Kasche, 1986; Terreni et al., 2005; Vera et al., 2017). Secondly, the kinetic analysis of sucrose

phosphorylase provides essential basis for design and optimization of the synthetic reaction for GG production, as follows.

Analyzing the reaction with sucrose and glycerol (Table 1), one recognizes that the kinetic fitness is higher for *Ba*SucP than *Lm*SucP. The higher transfer coefficient *TC* for *Ba*SucP derives mostly from a hydrolysis rate three-fold (= 2.68/0.88; Table 1) lower than for *Lm*SucP. Using 20 mM sucrose as the donor, one could do with a 1.74-fold (8.2/4.7; Table 1) lower glycerol concentration to achieve the same product selectivity GG/Glc. To have a selectivity of 10, one would need 1.2 M glycerol using *Ba*SucP.

The reaction with G1P has been challenging to use for GG synthesis. Thermodynamically, G1P is less preferred for glycosylation of glycerol than sucrose (Goedl et al., 2007). However, as has been shown for reactions of other phosphorylases, the reaction of G1P can be made quasi-irreversible through in situ product removal, using precipitation of the released phosphate in the presence of Mg^{2+} (Zhong, Luley-Goedl, & Nidetzky, 2019). Separation of GG from phosphate is readily achieved whereas separation from fructose is more difficult (Kruschitz & Nidetzky, 2020). Therefore, G1P remains an option for donor substrate. Kinetic models for *Ba*SucP and *Lm*SucP enable rigorous "window of operation" analysis to identify conditions suitable for the synthesis. We scanned [G1P] in the range 5–70 mM (*Lm*SucP) and 50–700 mM (*Ba*SucP) at glycerol concentrations varying between 0.85 and 2.0 M. We calculated the ν_X and ν_X/ν_H corresponding to each condition and defined the operational window according to the requirement that ν_X and ν_X/ν_H each be at least 80% of the maximum value. Within the window of operation (Figure S3), we identified the optimum point as involving the smallest [GOH]. For *Ba*SucP, we get [G1P] = 650 mM; [GOH] = 1.55 M; $\nu_X = 20.2\ s^{-1}$. For *Lm*SucP, we get [G1P] = 15 mM; [GOH] = 1.83 M; $\nu_X = 17.3\ s^{-1}$. *Ba*SucP is clearly preferred. Using *Lm*SucP, synthesis of GG in concentrations exceeding 15 mM should not be performed in batch. A fed-batch mode of reaction could be used in which 15 mM donor substrate is added according to progress of the reaction. However, a fed-batch process would involve substantially higher complexity due to the reaction control required. Evidently, it would be a highly laborious task to (try to) identify the respective windows of operation for *Ba*SucP and *Lm*SucP from experiments.

Although the underlying reasons may differ among different enzymes, the effect is common: it is true for numerous hydrolases that the efficiency of chemical group transfer is dependent on the type of donor substrate used (Fernandez-Lafuente et al., 1998; Kasche, 1986; Terreni et al., 2005; van Rantwijk et al., 1999; Vera et al., 2017). Glycoside hydrolases often can use a variety of donor substrates for hydrolysis (van Rantwijk et al., 1999; Vera et al., 2017; Zeuner et al., 2014). However, as shown for the β-glycosidase CelB from *Pyrococcus furiosus*, glycosyl transfer to acceptors from lactose is substantially less efficient when lactose is used compared to nitrophenyl-β-D-galactoside (Petzelbauer, Reiter, Splechtna, Kosma, & Nidetzky, 2000). Like most acid phosphatases, the G1P phosphatases from *E. coli* accepts a broad variety of donors for hydrolysis (e.g., nitrophenyl-phosphate, pyrophosphate) but transfer to acceptors is efficient only when G1P is used (Wildberger, Pfeiffer, Brecker, & Nidetzky, 2015; Wildberger, Pfeiffer, Brecker, Rechberger, et al., 2015). Even close homologues of G1P (e.g., α-D-mannose 1-phosphate) fail to elicit a similarly efficient transfer (unpublished results, 2020). The influence of the donor substrate is considerably more pronounced than in sucrose phosphorylase. Other phosphatases behave similarly (Han & Coleman, 1995; Tasnádi et al., 2020; van Herk, Hartog, van der Burg & Wever, 2005). Similar behavior has been noted for select esterases/lipases and proteases/N-acylases (Adlercreutz, 2017; Marsden et al., 2020; Müller et al., 2020). Extending previous studies, notably those on amidases and acyltransferases (Gololobov et al., 1988, 1990; Youshko et al., 2002), the kinetic framework analysis reported here could be useful in the study of these enzymes and group-transfer reactions catalyzed by them.

ACKNOWLEDGMENTS

This project has received funding from the European Union's Horizon 2020 research and innovation program under grant agreement no. 761030 (CARBAFIN).

DATA AVAILABILITY STATEMENT

Data obtained in the current study are available from the https://doi.org/10.5281/zenodo.3948424.

ORCID

Bernd Nidetzky http://orcid.org/0000-0002-5030-2643

REFERENCES

Adlercreutz, P. (2017). Comparison of lipases and glycoside hydrolases as catalysts in synthesis reactions. *Applied Microbiology and Biotechnology*, *101*(2), 513–519. https://doi.org/10.1007/s00253-016-8055-x

Asano, Y., Mihara, Y., & Yamada, H. (1999). A novel selective nucleoside phosphorylating enzyme from *Morganella morganii*. *Journal of Bioscience and Bioengineering*, *87*(6), 732–738. https://doi.org/10.1016/S1389-1723(99)80145-5

Beerens, K., De Winter, K., Van de Walle, D., Grootaert, C., Kamiloglu, S., Miclotte, L., … Desmet, T. (2017). Biocatalytic synthesis of the rare sugar kojibiose: Process scale-up and application testing. *Journal of Agricultural and Food Chemistry*, *65*(29), 6030–6041. https://doi.org/10.1021/acs.jafc.7b02258

Bolivar, J. M., Luley-Goedl, C., Leitner, E., Sawangwan, T., & Nidetzky, B. (2017). Production of glucosyl glycerol by immobilized sucrose phosphorylase: Options for enzyme fixation on a solid support and application in microscale flow format. *Journal of Biotechnology*, *257*, 131–138. https://doi.org/10.1016/j.jbiotec.2017.01.019

Bruggink, A., Roos, E. C., & de Vroom, E. (1998). Penicillin acylase in the industrial production of β-lactam antibiotics. *Organic Process Research & Development*, *2*(2), 128–133. https://doi.org/10.1021/op9700643

Cleland, W. W. (1975). Partition analysis and concept of net rate constants as tools in enzyme kinetics. *Biochemistry*, *14*(14), 3220–3224. https://doi.org/10.1021/bi00685a029

Dirks-Hofmeister, M. E., Verhaeghe, T., De Winter, K., & Desmet, T. (2015). Creating space for large acceptors: Rational biocatalyst design for resveratrol glycosylation in an aqueous system. *Angewandte Chemie International Edition*, *54*(32), 9289–9292. https://doi.org/10.1002/anie.201503605

Fernandez-Lafuente, R., Rosell, C. M., & Guisan, J. M. (1998). Modulation of the properties of penicillin G acylase by acyl donor substrates during N-protection of amino compounds. *Enzyme and Microbial Technology*, *22*(7), 583–587. https://doi.org/10.1016/S0141-0229(98)00239-7

Franceus, J., & Desmet, T. (2020). Sucrose phosphorylase and related enzymes in glycoside hydrolase family 13: Discovery, application and engineering. *International Journal of Molecular Sciences*, *21*(7), 2526. https://doi.org/10.3390/ijms21072526

Giordano, R. C., Ribeiro, M. P. A., & Giordano, R. L. C. (2006). Kinetics of β-lactam antibiotics synthesis by penicillin G acylase (PGA) from the viewpoint of the industrial enzymatic reactor optimization. *Biotechnology Advances*, *24*(1), 27–41. https://doi.org/10.1016/j.biotechadv.2005.05.003

Goedl, C., Sawangwan, T., Mueller, M., Schwarz, A., & Nidetzky, B. (2008). A high-yielding biocatalytic process for the production of 2-*O*-(α-D-glucopyranosyl)-*sn*-glycerol, a natural osmolyte and useful moisturizing ingredient. *Angewandte Chemie International Edition*, *47*(52), 10086–10089. https://doi.org/10.1002/anie.200803562

Goedl, C., Sawangwan, T., Wildberger, P., & Nidetzky, B. (2010). Sucrose phosphorylase: A powerful transglucosylation catalyst for synthesis of α-D-glucosides as industrial fine chemicals. *Biocatalysis and Biotransformation*, *28*(1), 10–21. https://doi.org/10.3109/10242420903411595

Goedl, C., Schwarz, A., Minani, A., & Nidetzky, B. (2007). Recombinant sucrose phosphorylase from *Leuconostoc mesenteroides*: Characterization, kinetic studies of transglucosylation, and application of immobilised enzyme for production of α-D-glucose 1-phosphate. *Journal of Biotechnology*, *129*(1), 77–86. https://doi.org/10.1016/j.jbiotec.2006.11.019

Goedl, C., Schwarz, A., Mueller, M., Brecker, L., & Nidetzky, B. (2008). Mechanistic differences among retaining disaccharide phosphorylases: Insights from kinetic analysis of active site mutants of sucrose phosphorylase and α,α-trehalose phosphorylase. *Carbohydrate Research*, *343*(12), 2032–2040. https://doi.org/10.1016/j.carres.2008.01.029

Gololobov, M. Y., Borisov, I. L., Belikov, V. M., & Švedas, V. K. (1988). Acyl group transfer by proteases forming acyl–enzyme intermediate: Kinetic model analysis. *Biotechnology and Bioengineering*, *32*(7), 866–872. https://doi.org/10.1002/bit.260320704

Gololobov, M. Y., Petrauskas, A., Pauliukonis, R., Koschke, V., Borisov, I. L., & Švedas, V. (1990). Increased nucleophile reactivity of amino acid β-naphthylamides in α-chymotrypsin-catalyzed peptide synthesis. *Biochimica et Biophysica Acta—Protein Structure and Molecular Enzymology*, *1041*(1), 71–78. https://doi.org/10.1016/0167-4838(90)90124-X

Han, R., & Coleman, J. E. (1995). Dependence of the phosphorylation of alkaline phosphatase by phosphate monoesters on the pKa of the leaving group. *Biochemistry*, *34*(13), 4238–4245. https://doi.org/10.1021/bi00013a013

Huber, R. E., Kurz, G., & Wallenfels, K. (1976). A quantitation of the factors which affect the hydrolase and transgalactosylase activities of β-galactosidase (*E. coli*) on lactose. *Biochemistry*, *15*(9), 1994–2001. https://doi.org/10.1021/bi00654a029

Ishikawa, K., Mihara, Y., Shimba, N., Ohtsu, N., Kawasaki, H., Suzuki, E.-I., & Asano, Y. (2002). Enhancement of nucleoside phosphorylation activity in an acid phosphatase. *Protein Engineering, Design and Selection*, *15*(7), 539–543. https://doi.org/10.1093/protein/15.7.539

Kasche, V. (1986). Mechanism and yields in enzyme catalysed equilibrium and kinetically controlled synthesis of β-lactam antibiotics, peptides and other condensation products. *Enzyme and Microbial Technology*, *8*(1), 4–16. https://doi.org/10.1016/0141-0229(86)90003-7

Kato, Y., Ooi, R., & Asano, Y. (1999). A new enzymatic method of nitrile synthesis by *Rhodococcus* sp. strain YH3-3. *Journal of Molecular Catalysis B: Enzymatic*, *6*(3), 249–256. https://doi.org/10.1016/S1381-1177(98)00080-0

Klotzsch, H., & Bergmeyer, H.-U. (1965). D-fructose. In H.-U. Bergmeyer (Ed.), *Methods of enzymatic analysis* (pp. 156–159). Cambridge, MA: Academic Press.

Kraus, M., Görl, J., Timm, M., & Seibel, J. (2016). Synthesis of the rare disaccharide nigerose by structure-based design of a phosphorylase mutant with altered regioselectivity. *Chemical Communications*, *52*(25), 4625–4627. https://doi.org/10.1039/C6CC00934D

Kruschitz, A., & Nidetzky, B. (2020). Removal of glycerol from enzymatically produced 2-α-D-glucosyl-glycerol by discontinuous diafiltration. *Separation and Purification Technology*, *241*, 116749. https://doi.org/10.1016/j.seppur.2020.116749

Luley-Goedl, C., & Nidetzky, B. (2010). Carbohydrate synthesis by disaccharide phosphorylases: Reactions, catalytic mechanisms and application in the glycosciences. *Biotechnology Journal*, *5*(12), 1324–1338. https://doi.org/10.1002/biot.201000217

Luley-Goedl, C., Sawangwan, T., Mueller, M., Schwarz, A., & Nidetzky, B. (2010). Biocatalytic process for production of α-glucosylglycerol using sucrose phosphorylase. *Food Technology and Biotechnology*, *48*(3), 276–283.

Marsden, S. R., Mestrom, L., McMillan, D. G. G., & Hanefeld, U. (2020). Thermodynamically and kinetically controlled reactions in biocatalysis—From concepts to perspectives. *ChemCatChem*, *12*(2), 426–437. https://doi.org/10.1002/cctc.201901589

Mestrom, L., Claessen, J. G. R., & Hanefeld, U. (2019). Enzyme-catalyzed synthesis of esters in water. *ChemCatChem*, *11*(7), 2004–2010. https://doi.org/10.1002/cctc.201801991

Mirza, O., Skov, L. K., Sprogøe, D., van den Brook, L. A. M., Beldman, G., Kastrup, J. S., & Gajhede, M. (2006). Structural rearrangements of sucrose phosphorylase from *Bifidobacterium adolescentis* during sucrose conversion. *Journal of Biological Chemistry*, *281*(46), 35576–35584. https://doi.org/10.1074/jbc.M605611200

Mueller, M., & Nidetzky, B. (2007). The role of Asp-295 in the catalytic mechanism of *Leuconostoc mesenteroides* sucrose phosphorylase probed with site-directed mutagenesis. *FEBS Letters*, *581*(7), 1403–1408. https://doi.org/10.1016/j.febslet.2007.02.060

Müller, H., Becker, A.-K., Palm, G. J., Berndt, L., Badenhorst, C. P. S., Godehard, S. P., … Bornscheuer, U. (2020). Sequence-based prediction of promiscuous acyltransferase activity in hydrolases. *Angewandte Chemie International Edition*, *59*(28), 11607–11612. https://doi.org/10.1002/anie.202003635

Norjannah, B., Ong, H. C., Masjuki, H. H., Juan, J. C., & Chong, W. T. (2016). Enzymatic transesterification for biodiesel production: A comprehensive review. *RSC Advances*, *6*(65), 60034–60055. https://doi.org/10.1039/C6RA08062F

Petzelbauer, I., Reiter, A., Splechtna, B., Kosma, P., & Nidetzky, B. (2000). Transgalactosylation by thermostable β-glycosidases from *Pyrococcus furiosus* and *Sulfolobus solfataricus*. *European Journal of Biochemistry*, *267*(16), 5055–5066. https://doi.org/10.1046/j.1432-1327.2000.01562.x

van Rantwijk, F., Woudenberg-van Oosterom, M., & Sheldon, R. A. (1999). Glycosidase-catalysed synthesis of alkyl glycosides. *Journal of Molecular Catalysis B: Enzymatic*, *6*(6), 511–532. https://doi.org/10.1016/S1381-1177(99)00042-9

Renirie, R., Pukin, A., van Lagen, B., & Franssen, M. C. R. (2010). Regio- and stereoselective glucosylation of diols by sucrose phosphorylase using sucrose or glucose 1-phosphate as glucosyl donor. *Journal of Molecular Catalysis B: Enzymatic*, *67*(3), 219–224. https://doi.org/10.1016/j.molcatb.2010.08.009

Schroën, C. G. P. H., Nierstrasz, V. A., Moody, H. M., Hoogschagen, M. J., Kroon, P. J., Bosma, R., … Tramper, J. (2001). Modeling of the enzymatic kinetic synthesis of cephalexin—Influence of substrate concentration and temperature. *Biotechnology and Bioengineering*, *73*(3), 171–178. https://doi.org/10.1002/bit.1049

Segel, I. H. (1993). *Enzyme kinetics: Behavior and analysis of rapid equilibrium and steady-state enzyme systems*. New York, NY: John Wiley & Sons.

Seibel, J., Jördening, H.-J., & Buchholz, K. (2006). Glycosylation with activated sugars using glycosyltransferases and transglycosidases. *Biocatalysis and Biotransformation*, *24*(5), 311–342. https://doi.org/10.1080/10242420600986811

Sio, C. F., & Quax, W. J. (2004). Improved β-lactam acylases and their use as industrial biocatalysts. *Current Opinion in Biotechnology*, *15*(4), 349–355. https://doi.org/10.1016/j.copbio.2004.06.006

Sklyarenko, A. V., El'darov, M. A., Kurochkina, V. B., & Yarotsky, S. V. (2015). Enzymatic synthesis of β-lactam acids (review). *Applied Biochemistry and Microbiology*, *51*(6), 627–640. https://doi.org/10.1134/S0003683815060150

Sprogøe, D., van den Broek, L. A. M., Mirza, O., Kastrup, J. S., Voragen, A. G. J., Gajhede, M., & Skov, L. K. (2004). Crystal structure of sucrose phosphorylase from *Bifidobacterium adolescentis*. *Biochemistry*, *43*(5), 1156–1162. https://doi.org/10.1021/bi0356395

Subileau, M., Jan, A. H., Drone, J., Rutyna, C., Perrier, V., & Dubreucq, E. (2017). What makes a lipase a valuable acyltransferase in water abundant medium? *Catalysis Science & Technology*, *7*(12), 2566–2578. https://doi.org/10.1039/C6CY01805J

Tasnádi, G., Staśko, M., Ditrich, K., Hall, M., & Faber, K. (2020). Preparative-scale enzymatic synthesis of *rac*-glycerol-1-phosphate from crude glycerol using acid phosphatases and phosphate. *ChemSusChem*, *13*(7), 1759–1763. https://doi.org/10.1002/cssc.201903236

Terreni, M., Tchamkam, J. G., Sarnataro, U., Rocchietti, S., Fernández-Lafuente, R., & Guisán, J. M. (2005). Influence of substrate structure on PGA-catalyzed acylations. Evaluation of different approaches for the enzymatic synthesis of cefonicid. *Advanced Synthesis & Catalysis*, *347*(1), 121–128. https://doi.org/10.1002/adsc.200404136

van den Broek, L. A. M., van Boxtel, E. L., Kievit, R. P., Verhoef, R., Beldman, G., & Voragen, A. G. J. (2004). Physico-chemical and transglucosylation properties of recombinant sucrose phosphorylase from *Bifidobacterium adolescentis* DSM20083. *Applied Microbiology and Biotechnology*, *65*(2), 219–227. https://doi.org/10.1007/s00253-003-1534-x

van Herk, T., Hartog, A. F., van der Burg, A. M., & Wever, R. (2005). Regioselective phosphorylation of carbohydrates and various alcohols by bacterial acid phosphatases; Probing the substrate specificity of the enzyme from *Shigella flexneri*. *Advanced Synthesis & Catalysis*, *347*(7-8), 1155–1162. https://doi.org/10.1002/adsc.200505072

Vera, C., Guerrero, C., Aburto, C., Cordova, A., & Illanes, A. (2020). Conventional and non-conventional applications of β-galactosidases. *Biochimica et Biophysica Acta—Proteins and Proteomics*, *1868*(1), 140271. https://doi.org/10.1016/j.bbapap.2019.140271

Vera, C., Guerrero, C., Wilson, L., & Illanes, A. (2017). Optimization of reaction conditions and the donor substrate in the synthesis of hexyl-β-D-galactoside. *Process Biochemistry*, *58*, 128–136. https://doi.org/10.1016/j.procbio.2017.05.005

Verhaeghe, T., De Winter, K., Berland, M., De Vreese, R., D'hooghe, M., Offmann, B., & Desmet, T. (2016). Converting bulk sugars into prebiotics: Semi-rational design of a transglucosylase with controlled selectivity. *Chemical Communications*, *52*(18), 3687–3689. https://doi.org/10.1039/C5CC09940D

Wildberger, P., Luley-Goedl, C., & Nidetzky, B. (2011). Aromatic interactions at the catalytic subsite of sucrose phosphorylase: Their roles in enzymatic glucosyl transfer probed with Phe52 → Ala and Phe52 → Asn mutants. *FEBS Letters*, *585*(3), 499–504. https://doi.org/10.1016/j.febslet.2010.12.041

Wildberger, P., Pfeiffer, M., Brecker, L., & Nidetzky, B. (2015). Diastereoselective synthesis of glycosyl phosphates by using a phosphorylase–phosphatase combination catalyst. *Angewandte Chemie International Edition*, *54*(52), 15867–15871. https://doi.org/10.1002/anie.201507710

Wildberger, P., Pfeiffer, M., Brecker, L., Rechberger, G. N., Birner-Gruenberger, R., & Nidetzky, B. (2015). Phosphoryl transfer from α-D-glucose 1-phosphate catalyzed by *Escherichia coli* sugar-phosphate phosphatases of two protein superfamily types. *Applied and Environmental Microbiology*, *81*(5), 1559–1572. https://doi.org/10.1128/aem.03314-14

Youshko, M. I., Chilov, G. G., Shcherbakova, T. A., & Švedas, V. K. (2002). Quantitative characterization of the nucleophile reactivity in penicillin acylase-catalyzed acyl transfer reactions. *Biochimica et Biophysica Acta—Proteins and Proteomics*, *1599*(1), 134–140. https://doi.org/10.1016/S1570-9639(02)00413-2

Zeuner, B., Jers, C., Mikkelsen, J. D., & Meyer, A. S. (2014). Methods for improving enzymatic trans-glycosylation for synthesis of human milk oligosaccharide biomimetics. *Journal of Agricultural and Food Chemistry*, *62*(40), 9615–9631. https://doi.org/10.1021/jf502619p

Zhong, C., Luley-Goedl, C., & Nidetzky, B. (2019). Product solubility control in cellooligosaccharide production by coupled cellobiose and cellodextrin phosphorylase. *Biotechnology and Bioengineering*, *116*(9), 2146–2155. https://doi.org/10.1002/bit.27008

SUPPORTING INFORMATION

Additional supporting information may be found online in the Supporting Information section.

How to cite this article: Klimacek M, Sigg A, Nidetzky B. On the donor substrate dependence of group-transfer reactions by hydrolytic enzymes: Insight from kinetic analysis of sucrose phosphorylase-catalyzed transglycosylation. *Biotechnology and Bioengineering*. 2020;117:2933–2943. https://doi.org/10.1002/bit.27471